Heliyon 5 (2019) e01720

Contents lists available at ScienceDirect

Heliyon

journal homepage: www.heliyon.com

Carbon steel corrosion controlled by vegetable polyol phosphate, in medium containing chloride and glyoxal: influence of phosphate content and CO_2

Rita Cristina da Silva, Melissa Heinen, Gabriel A. Lorenzi, Demétrius W. Lima, João Henrique Lingner Moura, Jamili M. de Freitas, Emilse M.A. Martini, Cesar L. Petzhold *

Institute of Chemistry, UFRGS, Av. Bento Gonçalves, 9500, Porto Alegre, 91501-970, P.O.Box 15003, Brazil

ARTICLE INFO

Keywords:
Materials science
Electrochemistry

ABSTRACT

Glyoxal is a potential sequestrant of H_2S in the pre-salt exploration. However, the mixture containing packer fluid and glyoxal is corrosive. The addition of an eco-friendly polyol phosphate acts as corrosion inhibitor of the AISI 1020 in this environment. The objective of the present work was to study the influence of phosphate content in the inhibitor formulation, as well as its action in packer fluid and glyoxal solution in the presence of dissolved CO_2, by means of surface analysis and electrochemical measurements. The results demonstrated that the inhibition efficiency increases as the phosphate content increases. In the beginning of the tests, the polarization resistance increases from 2.2 kΩ cm^2 (2.5 % phosphate) to 11.2 kΩ cm^2 (10 % phosphate). In CO_2 – containing medium, 500 ppm dosage of polyol phosphate increases the polarization resistance (from 0.35 kΩ cm^2 to 5.9 kΩ cm^2) and decreases both the capacitance (from 111.5 μF cm^{-2} to 10.2 μF cm^{-2}) and the corrosion current (in 67%). Polyol phosphate is effective as corrosion inhibitor in the presence of CO_2 due to its adsorption on the metal surface or on the film of the previously formed oxide.

1. Introduction

Carbon steel is one of the materials utilized in the construction of oil and gas pipelines [1,2]. In oil industry, CO_2 injection is frequently used in oil retrieval [3]. The resulting water contains CO_2 and, routinely, can be recycled for injection in order to increase the reservoir pressure, also enabling advanced oil recovery [4]. In very deep waters the CO_2 reaches high concentration levels (10–40% v/v), the same happening with hydrogen sulfide (H_2S), which is extremely toxic [5,6].

Dry CO_2 gas is not corrosive at usual transport temperatures in oil and gas producing systems. However, when CO_2 is dissolved in water, there is carbonic acid formation (H_2CO_3) in the aqueous phase, which causes iron oxidation and cathodic release of hydrogen in acid solutions. The nature of the corrosion caused by CO_2 varies according to specific environmental conditions, with temperature and pressure of CO_2 standing out in this corrosion process [7]. With regard to deep waters, like, for instance, the pre-salt oil exploration in Brazil [8], in addition to the high concentrations of the gases CO_2 and H_2S [9], the presence of chloride in both water injection and packer fluid constitute a more critical situation to corrosion [10,11]. Hydrogen sulfide has been mitigated by chemical agents, which convert it into inert or less toxic products. Glyoxal is a molecule that can be used as potential H_2S removal agent, notwithstanding its extremely corrosive effect on carbon steel [12].

New green corrosion inhibitors, synthesized from renewable and environmentally friendly sources, are continuously researched. The study of the mechanism of action, forming a barrier layer against the corrosive processes, includes the determination of the type of adsorption isotherm. Theoretical investigations based on Monte Carlo, molecular dynamics and quantum mechanics techniques are also carried out and confirm the adsorption of the green inhibitors on the metallic substrate, through electron donor-acceptor interactions in their reactive sites [13, 14, 15, 16, 17, 18]. Corrosion inhibitors synthesized from renewable sources are widely used to minimize CO_2 corrosion in oil and gas industry [19]. Due to its biodegradability, vegetable oils derivatives, plant extracts such as tannin and aminoacids are considered green corrosion inhibitors and they have been reported as corrosion inhibitors for a diversity of metals in various aggressive media [20, 21, 22, 23, 24, 25, 26, 27, 28, 29, 30, 31, 32]. Recently, inhibitors based on tetraphosphonic acid lessened carbon steel susceptibility to corrosion in 3% NaCl aqueous solution [33, 34, 35]. Inhibition action was promoted by adsorption of monophosphonates molecules on the carbon steel surface, forming a protective film that adheres to the metal surface and works as a barrier against chloride ions

* Corresponding author.
E-mail address: petzhold@iq.ufrgs.br (C.L. Petzhold).

https://doi.org/10.1016/j.heliyon.2019.e01720
Received 9 November 2018; Received in revised form 22 April 2019; Accepted 9 May 2019

attack [36, 37, 38]. Phosphorus-based derivatives pose a considerable challenge and present great interest in the field of environmental remediation [33, 39, 40, 41, 42]. However, the performance of molecules that present corrosion inhibition has not been reported when it comes to media containing CO_2, chloride and glyoxal.

Our research group has proposed a new environmentally friendly corrosion inhibitor based on polyol phosphate, obtained from epoxidized soybean oil and further reaction with phosphoric acid. The obtained molecule possesses a hydrophilic moiety, composed of phosphate functional group, and a hydrophobic moiety, constituted of hydrocarbons backbone.

Fig. 1 depicts a possible structure for the obtained polyol phosphate. The hydrophilic moiety is chemically adsorbed on passive oxide film of carbon steel, via oxygen vacancies, whereas the hydrophobic moiety constitutes a physical barrier against the entry of chloride [43]. In this study, the evaluation was focused on the effect of the number of phosphate groups attached to the hydrocarbon chain on the inhibitor efficiency. It was also verified the action of this molecule in AISI 1020 carbon steel corrosion control, in medium containing high contents of chloride and glyoxal, in saturated CO_2 solution, by means of electrochemical impedance spectroscopic techniques and polarization curves for Tafel analysis.

2. Materials and methods

2.1. Inhibitor synthesis

Polyol phosphate was synthesized in our research laboratory according to a previously described procedure [43, 44], using two different H_3PO_4 concentrations for the phosphatization. The characterization of the product obtained was performed by ^{1}H-NMR. Acidity index and hydroxyl content were also determined. The results obtained for both syntheses are presented on Table 1.

Size exclusion chromatography analyses (SEC) were performed in tetrahydrofuran (THF) at 45 °C and a flow rate of 1 mL/min using a Viscotek system comprising of a GPCmax VE-2001 module (pump, degasser, and auto-injector) and a TDA-302 oven-multi-detector unit (UV, RI, Viscometer, and Light Scattering). The system was equipped with a KF-G guard column followed by four KF-series Shodex columns (806M, 805L, 804L, and 803L). Molar mass averages were calculated using the RI signal and a calibration curve based on narrow polystyrene standards ranging 0.5 to 4 $\times$ 10^3 kg mol^{-1}. The results indicated the presence of molecules with lower molar mass, which were found to average about 350 g mol^{-1} [44]. In order to render the new inhibitor compatible with the high salinity system (packer fluid), a modification was necessary in the synthesized polyol by means of its neutralization until reaching a slightly alkaline pH (pH 8.2). In view of this, 2.0244 g of polyol phosphate were dissolved in 25 mL of ether and ethanol solution (2:1, v/v). Shortly after that, a titration with 0.01 mol L^{-1} NaOH was carried out using 1% phenolphthalein (alcoholic) as indicator until reaching the first color change for neutralization and obtaining a soluble product in packer fluid.

Table 1
Characterization of synthesized polyol phosphate samples.

Polyol Phosphate	Acidity Index (mg KOH g^{-1})	Hydroxyl Content (mg KOH g^{-1})
2.5% H_3PO_4	30.87	145.68
10% H_3PO_4	124.68	53.7

2.2. Chemicals

The packer fluid solution was obtained by preparing a 6 mol L^{-1} NaCl solution (analytical grade/Nuclear) in deionized water. Density and pH were adjusted with NaOH solution (25%) until reaching final density of 1.186 g cm^{-3} and pH between 7 and 8, in compliance with the recommendations for completion fluid [45]. Glyoxal was used in aqueous solution (Basf), commercial grade, with 39.5-40.5% concentration, pH 2.0-3.5 and density of 1.27 g cm^{-3} at 20 °C. Starting from these solutions, mixtures of packer fluid and glyoxal (1:1, v/v) were prepared with and without addition of corrosion inhibitor at the

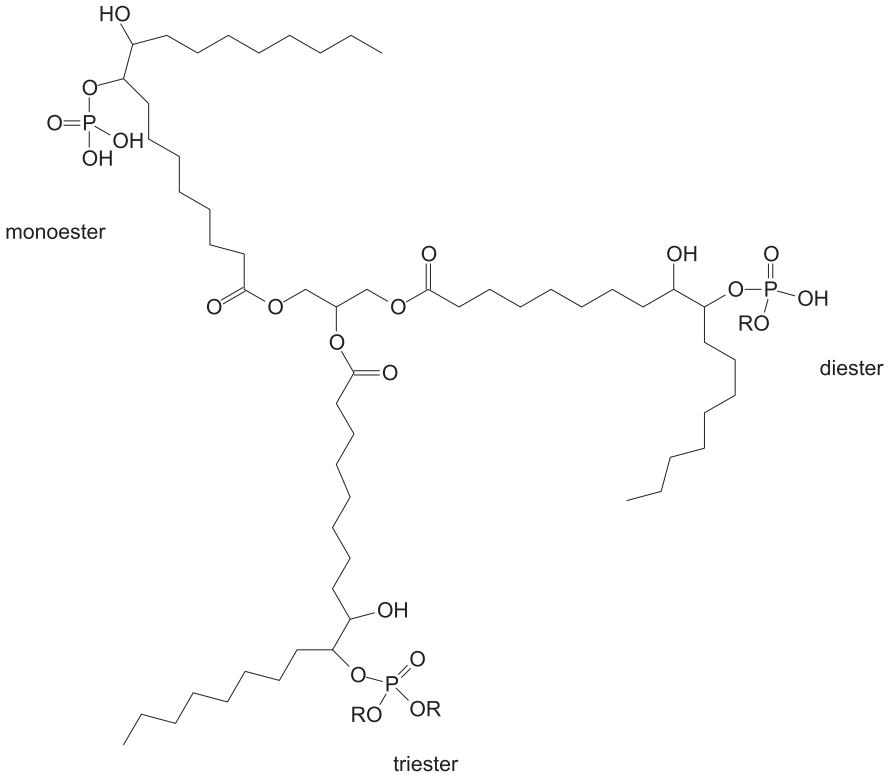

Fig. 1. Triacylglycerol showing the possible structure of the polyol phosphate derivatives: monoester, diester and triester (R = alkyl group).

concentration of 500 ppm with formulation based on polyol phosphate. In this mixture, the chloride concentration is reduced to 3 mol L^{-1} and glyoxal to 20 % volume.

2.3. Electrochemical measurements

Electrochemical experiments were performed in a conventional three-electrode cell: saturated calomel electrode (SCE) as a reference to which all potentials are referred, platinum wire as counter electrode and, as working electrode, AISI 1020 carbon steel coupons (dimensions: 4 cm × 1.3 cm x 1 mm). The composition of the AISI 1020 carbon steel is (wt. %): 0.0830 C, 0.2130 Mn, 0.0160 P, 0.0130 S, 0.0120 Si, 0.0120 Cu, 0.0050 Ni, 0.0180 Cr, 0.0030 Mo, 0.0050 Sn, 0.0410 Al, 0.0038 N, 0.0030 Nb, 0.0010 V, 0.0110 Ti, 0.0035 B and balance Fe. The coupons were polished with #400, #600 and #1200 sandpapers and washed with distilled water and alcohol. In order to insulate the area exposed to the solution, commercial paint for metals was used (red oxide primer, anti-corrosive). A rectangular area of approximately 1 cm^2 was left uncovered, whereas the remaining part was completely painted.

Electrochemical Impedance Spectroscopy (EIS) measurements were performed in a potentiostat coupled to a Frequency Response Analyzer (FRA) from Autolab, software version 4.8, interfaced with a computer, at the corrosion potential (E_{corr}) by applying a 10 mV amplitude sinusoidal wave, in the frequency range between 100 kHz and 100 mHz. For each sample, 10 frequency values per decade were analyzed. Potentiodynamic polarization curves were obtained in the same potentiostat, with 0.001 V s^{-1} potential scan rate in the potential range between -1.2 V_{SCE} and + 0.5 V_{SCE}. The experiments were carried out over different times of immersion. SEM measurements of the AISI 1020 carbon steel coupons were carried out after 24 h of immersion in packer fluid and glyoxal mixtures without or with polyol phosphate corrosion inhibitor and with or without CO_2.

3. Results and discussion

In a work formerly published by our research group [43], electrochemical impedance spectroscopy assays at the corrosion potential, over the immersion time, proved that polyol phosphate inhibits AISI 1020 carbon steel corrosion in packer fluid medium. This property was confirmed by the increase in polarization resistance and decrease in capacitance, indicating the presence of a film over the metal surface that acts as a barrier against chloride attack. The decrease in capacitance with the increasing concentration of the inhibitor enabled to substantiate that the adsorption mechanism follows the Langmuir isotherm. The high value of K_{ads} (1553.87) indicated that the inhibitor desorption is not favored. The high negative value of ΔG° (-28.14 kJ mol^{-1}) demonstrated a complex physicochemical interaction between the inhibitor molecules and the metal surface. Phosphate groups are chemically adsorbed through oxygen vacancies of the oxide film, while the hydrocarbon chain forms a hydrophobic barrier that hinders the intrusion of the chloride-containing electrolyte. When commercial grade glyoxal was mixed with the packer fluid, forming a 50% v/v solution, impedance assays for AISI 1020 carbon steel at the corrosion potential over the immersion time demonstrated that R_p is diminished and C is increased, but in a more marked way in the medium without inhibitor, so that the degree of surface coverage, in the presence of the inhibitor, remains constant (0.86 ± 0.010). In Tafel analysis, the values of E_{corr} are greater and those of i_{corr} are smaller in the presence of the inhibitor, regardless the immersion time. It was also verified that Tafel constants (b_a and b_c) are greater in the presence of the inhibitor, attesting to its characteristic as a mixed-type corrosion inhibitor, that is, which is adsorbed indistinctively on both cathodic and anodic regions.

The electrochemical assays already published [43] were carried out in the absence of inhibitor and in the presence of 500 ppm inhibitor synthesized with 10 % H_3PO_4. In order to confirm that the phosphate group bonded to the hydrocarbon chain plays an important role in attaching the inhibitor to the oxide coating vacancies initially present in in the carbon steel, electrochemical impedance assays were carried out over the immersion time, under the same conditions, but using polyol phosphate-based inhibitor obtained from 2.5% H_3PO_4.

Fig. 2 shows the impedance diagrams obtained for AISI 2010 carbon steel in polyol-containing medium, with 2.5 % H_3PO_4. The Nyquist plots (Fig. 2a) present an incomplete capacitance arc that represents the metal/film/solution interface. As for Bode plots, the diagrams show (Fig. 2b) a high frequency flat region, which represents R_s, the solution resistance in the vicinity of the carbon steel electrode, and a sloped straight line at intermediate frequency, related to the metal/film/solution interface capacitance, which changes the slope at low frequency. In this region, the impedance is related to R_p, the polarization resistance at the metal/film interface. Values of R_s, R_p and C were evaluated by fitting the experimental data with de equivalent circuit [$R_s(R_pC)$]. Surface coverage fraction θ was determined by comparing metal/solution interface capacitances in the presence and in the absence of inhibitor, by means of [46]:

$$\frac{C}{C^o} = \frac{A_{inh}}{A^o} = \frac{1-\theta}{1} \quad (1)$$

In which C and C^o correspond to metal/solution interface capacitance with and without inhibitor, respectively.

Table 2 shows the results along with the systems without inhibitor and with polyol-based inhibitor with 10 % H_3PO_4 [43]. Intermediate values lying between the system without inhibitor and with inhibitor in 10 % H_3PO_4 where observed.

The presence of polyol phosphate at the proportion of 2.5 % in H_3PO_4 did not bring about significant changes in E_{corr} in relation to the system without inhibitor. Values between -656 mV_{ECS} (= -414 mV_{ENH}) and -611 mV_{ECS} (= -369 mV_{ENH}) correspond, in Pourbaix diagram for iron, to the steel passivated with a double oxide of Fe(II) and Fe(III), like a spinel structure. However, R_p is greater than in the medium without inhibitor, indicating that polyol acts already as a barrier that hinders the corrosion process. The inhibiting effect is also substantiated by smaller capacitance values in relation to the medium without inhibitor. Along the immersion time, R_p decreases and C increases, but in a less drastic way than in the absence of inhibitor. The degree of surface coverage θ, calculated for this phosphate content, is smaller than that for the inhibitor with 10 % H_3PO_4. This indicates the presence of a less stabilized oxide film, which does not cover the entire metal surface, leaving anodic and cathodic regions exposed and allowing iron oxidation. The results point to an important role played by phosphate anion in the chemical adhesion of the inhibitor to the oxygen vacancies of iron oxide, leading to a greater stabilization of the passivation oxide. The greater the number of phosphate anions binded to the hydrocarbon chain, the greater the polarization resistance, the smaller the capacitance and the greater the degree of metal surface coverage. This tendency continues, even after 14 days of immersion. The results denote the role played by phosphate in promoting the iron oxide film stabilization by chemical adsorption, through the bonding of the oxygen binded to phosphorus and the oxygen vacancies of the defective oxide film. Consequently, the greater the number of phosphate groups, the more adherent is the molecule and the greater its barrier effect against corrosion.

In oil industry, the gas CO_2 may be present dissolved in oil. The corrosion caused by CO_2 leads to the deterioration of both equipment and carbon steel pipelines, resulting in accidents and high costs. For this reason, the influence of CO_2 on the polyol phosphate inhibition efficiency was verified in packer fluid and glyoxal medium. AISI 1020 carbon steel coupons were left immersed in a mixture of packer fluid and glyoxal, with and without inhibitor, during 24 h with CO_2-gas bubbling. For the tests with CO_2, the formulation with 10 % H_3PO_4 was used. Subsequently, the bubbling process was halted and experiments of electrochemical impedance spectroscopy and linear voltammetry were carried out.

Fig. 3 (a and b) present the impedance results obtained in the presence and in the absence of polyol phosphate inhibitor. In the absence of

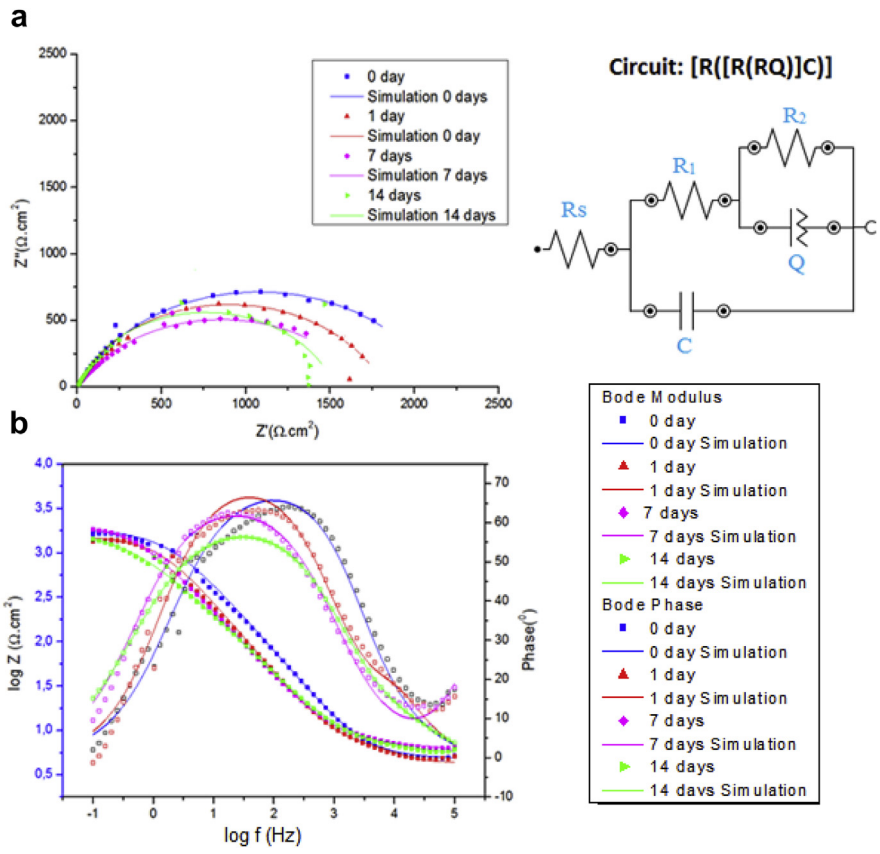

Fig. 2. Nyquist (2a) and Bode (2b) impedance plots for AISI 1020 carbon steel in different times of immersion in packer fluid (50 %) and glyoxal (50 %) mixtures with 500 ppm of polyol phosphate at E_{corr}. pH 7.4. H_3PO_4 content = 2.5 %.

inhibitor, Nyquist diagram shows a capacitive loop, which represents the metal/solution interface, characterized by solution resistance (R_s), electric double layer capacitance (C) and polarization resistance (R_p). In Bode plots, R_s and R_p are determined in the flat portions of high and low frequencies respectively, separated by the sloping straitght line in the intermediate frequency range, which represents capacitance C. When the inhibitor is added to the medium, the capacitive arc increases its diameter and it is incomplete at low frequencies, thus indicating a greather capacitive effect of dielectric barrier. The same result is ascertained by means of Bode plots, with capacitive straight line being pratically prevalent throughout the frequency range in which the impedance was assessed. This result indicates the presence of a protective layer between the metal surface and the solution. In the absence of inhibitor, the pre-existent oxide film, formed during the preparation of the working electrode, is not stable, undergoing dissolution and not imparting protection.

The chemical reactions involved are [7, 47, 48, 49]:

a) Reactions that occur in the solution:

$$CO_{2(g)} \rightleftharpoons CO_{2(aq)} \quad (2)$$

$$CO_{2(aq)} + H_2O \rightleftharpoons H_2CO_{3(aq)} \quad (3)$$

$$H_2CO_{3(aq)} \rightleftharpoons H^+ + HCO_3^- \quad (4)$$

$$HCO_3^- \rightleftharpoons H^+ + CO_3^{2-} \quad (5)$$

b) Mass transfer of the corrosive species to the steel surface:

Table 2
Comparison of electrochemical impedance spectroscopy data for AISI 1020 carbon steel in different times of immersion in packer fluid and glyoxal mixtures without and with 500 ppm of polyol phosphate at E_{corr}. pH = 7.4, with 2.5 % or 10 % of H_3PO_4.

Day	H_3PO_4 (%)	$C_{inhibitor}$ (ppm)	E_{corr} (mV_{ECS})	R_s(Ω cm^2)	R_p (kΩ cm^2)	C (μF cm^{-2})	θ
0		0	-664 ± 10	5.1 ± 0.5	1.6 ± 0.2	59.3 ± 14.2	
	2.5	500	-656 ± 14	5.3 ± 0.5	2.2 ± 0.4	10.3 ± 1.2	0.83 ± 0.01
	10	500	-460 ± 18	5.7 ± 0.2	11.2 ± 0.4	7.9 ± 1.0	0.87 ± 0.01
1		0	-644 ± 11	5.3 ± 0.7	0.7 ± 0.2	71.6 ± 18.2	
	2.5	500	-640 ± 4	5.2 ± 0.3	2.1 ± 0.4	15.3 ± 5.7	0.79 ± 0.03
	10	500	-526 ± 8	6.2 ± 0.7	10.7 ± 0.8	10.3 ± 2.2	0.86 ± 0.01
7		0	-629 ± 7	6.0 ± 1.0	0.5 ± 0.2	87.5 ± 27.5	
	2.5	500	-628 ± 5	6.8 ± 0.5	2.0 ± 0.3	17.3 ± 8.7	0.80 ± 0.02
	10	500	-562 ± 10	6.4 ± 0.5	5.7 ± 0.9	12.8 ± 2.4	0.85 ± 0.02
14		0	-612 ± 4	4.7 ± 0.4	0.3 ± 0.1	108.1 ± 22.6	
	2.5	500	-611 ± 10	6.2 ± 0.6	1.6 ± 0.4	18.7 ± 5.2	0.83 ± 0.01
	10	500	-581 ± 12	6.0 ± 0.4	2.4 ± 0.8	14.4 ± 3.3	0.87 ± 0.01

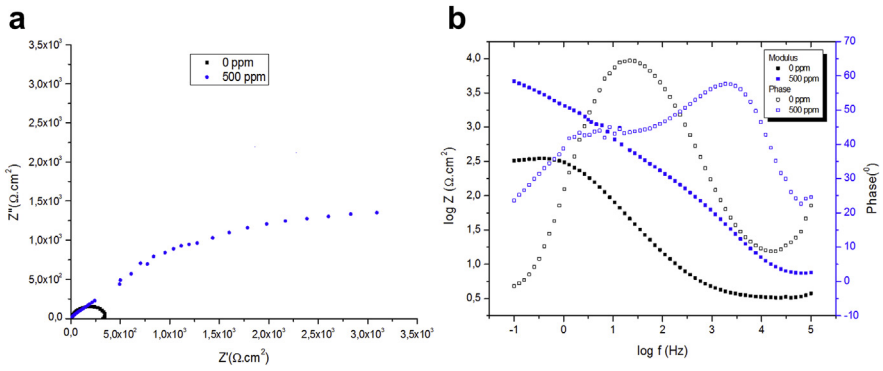

Fig. 3. Nyquist (3a) and Bode (3b) impedance plots for AISI 1020 carbon steel after 24 h of immersion in packer fluid (50 %) and glyoxal (50 %) mixtures with or without 500 ppm of polyol phosphate at E_{corr}, with CO_2 bubbling.

Table 3
Comparison of electrochemical impedance spectroscopy data for AISI 1020 carbon steel in packer fluid and glyoxal mixtures without and with 500 ppm of polyol phosphate at E_{corr}. Influence of CO_2.

CO_2	$C_{inhibitor}$ (ppm)	E_{corr} (mV_{ECS})	R_s (Ω cm^2)	R_p ($k\Omega$ cm^2)	C (μF cm^{-2})	θ	φ(%)
without	0	-644 ± 11	5.3 ± 0.7	0.70 ± 0.2	71.6 ± 18.2		
with	0	-674 ± 10	3.2 ± 1.1	0.35 ± 0.1	111.5 ± 23.2		
without	500	-526 ± 8	6.2 ± 0.7	10.7 ± 0.8	10.3 ± 2.2	0.86 ± 0.01	93 ± 1
with	500	-534 ± 10	5.3 ± 0.3	5.9 ± 0.5	10.2 ± 1.0	0.91 ± 0.01	94 ± 1

$$H^+_{(sol)} \rightarrow H^+_{(surface)} \quad (6)$$

$$H_2CO_{3(sol)} \rightarrow H_2CO_{3(surface)} \quad (7)$$

$$HCO^-_{3(sol)} \rightarrow HCO^-_{3(surface)} \quad (8)$$

$$CO^{2-}_{3\,(sol)} \rightarrow CO^{2-}_{3\,(surface)} \quad (9)$$

c) Chemical reactions on the steel surface:

Cathodic reactions:

$$2\ H_2CO_{3(aq)} + 2\ e^- \rightarrow H_2 + 2\ HCO^-_3 \quad (10)$$

$$2\ HCO^-_3 + 2\ e^- \rightarrow H_2 + 2\ CO^{2-}_3 \quad (11)$$

$$2\ H^+ + 2\ e^- \rightarrow H_2 \quad (12)$$

Anodic reactions:

$$Fe_{(s)} \rightarrow Fe^{2+}_{(aq)} + 2\ e^- \quad (13)$$

d) Precipitation of corrosion products:

$$Fe^{2+} + 2\ HCO^{-2}_3 \rightarrow Fe(HCO_3)_{2\ (s)} \quad (14)$$

$$Fe(HCO_3)_{2\ (s)} \rightarrow FeCO_{3(s)} + CO_2 + H_2O \quad (15)$$

$$Fe^{2+} + CO^{-2}_3 \rightarrow FeCO_{3\ (s)} \quad (16)$$

In CO_2-saturated aqueous medium, the corrosion product generated is iron (II) carbonate, which has low solubility (solubility = 5.6×10^{-6} M at 25 °C). This salt precipitates over the steel surface, when the concentration of Fe^{2+} and CO^{2-}_3 exceeds the solubility limit in the aqueous solution close to the metal, forming a film of corrosion products that works as a barrier, which isolates the steel from the aggressive medium. However, film stability depends on the pH of the medium. In acid pH, the film is partially dissolved and loses its protective properties. In addition, regardless the pH, the film of corrosion products is porous and aggressive anions can pass through it and react with the metal matrix. Chloride anions are preferably adsorbed onto the metal surface in relation to HCO^-_3 or CO^{2-}_3, thus impairing $FeCO_3$ formation [47].

In a medium with inhibitor, the previous oxide film is stabilized by the chemical adsorption of oxygen from the phosphate group on the oxide defects and by the physical adsorption of the inhibitor non-polar moiety. This protective coating hinders the chloride effect.

Table 3 shows a comparison of impedance parameters obtained from Nyquist (R_s and R_p) and Bode (C), and also the steel surface coverage fraction (θ) (Eq. 1), for the systems with and without inhibitor (500 ppm), and with or without CO_2-gas bubbling. In the absence of inhibitor, R_S is smaller in the CO_2-containing solution in relation to the solution without CO_2. In the presence of CO_2 there is formation of H_2CO_3 (Eqs. (2) and (3)), a weak acid that ionizes as described in Eqs. (4) and (5). The ionization increases the solution conductivity and the resistante R_s decreases. E_{corr} and R_p undergo reduction, whereas C is enhanced, indicating that, in the presence of CO_2, the solution is more corrosive, since the oxidation reaction is improved. With CO_2 bubbling and carbonic acid formation, the pH of the solution drops from 7.4 to 5.6. In acid medium, the corrosion product $FeCO_3$ is soluble, resulting in a porous oxide that

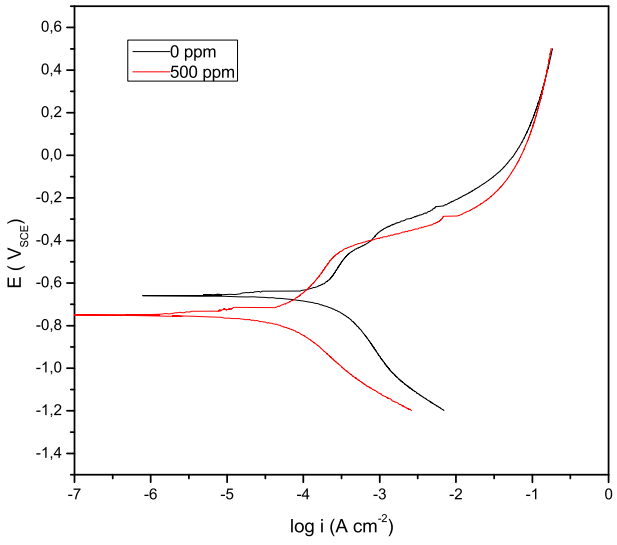

Fig. 4. Tafel plots for AISI 1020 carbon steel after 24 h of immersion in packer fluid (50 %) and glyoxal (50 %) mixtures with or without 500 ppm of polyol phosphate. v = 0.001 V s^{-1}. Influence of CO_2.

Table 4
Comparison of electrochemical corrosion data for AISI 1020 carbon steel after 24 h of immersion packer fluid and glyoxal mixtures without and with 500 ppm of polyol phosphate. Influence of CO_2.

CO_2	$C_{inhibitor}$ (ppm)	E_{corr} (mV_{SCE})	i_{corr} ($\mu A\ cm^{-2}$)	b_a ($mV\ dec^{-1}$)	$-b_c$ ($mV\ dec^{-1}$)
without	0	-736 ± 25	12.0 ± 2.8	70 ± 11	53 ± 11
with	0	-674 ± 13	15.9 ± 0.8	42 ± 8	43 ± 7
without	500	-758 ± 22	3.8 ± 0.9	109 ± 12	116 ± 11
with	500	-752 ± 18	5.2 ± 0.5	72 ± 11	44 ± 2

imparts protection to the carbon steel against chloride attack. In the presence of polyol phosphate-based inhibitor, impedance parameters change drastically. Regardless the presence of CO_2, E_{corr} is greater, thus pointing to the presence of a protective oxide film or cathodic sites deactivation, leading to metal protection. R_s is smaller in medium with both inhibitor and CO_2 due to the increment of the ionic concentration related to the presence os ions H^+, HCO_3^- and CO_3^{2-}. R_p is greater in medium with inhibitor, regardless the presence of CO_2. Nevertheless, even with high value, R_p diminishes as CO_2 is bubbled. The remarkable fact is the small capacitance value, in comparison with the absence of inhibitor, and that is not affected neither by CO_2 nor by the pH of the medium. This indicates the presence of a physical barrier between the carbon steel and the solution, with high coverage fraction. Inhibiton efficiency (φ) was calculated from R_p values, using:

$$\varphi = \left(\frac{R_p - R_p^o}{R_p}\right) x\ 100 \quad (17)$$

In which R_p and R_p^o represent polarization resistance in the presence and in the absence of inhibitor, respectively. The values of φ are shown on Table 3 and indicate that the inhibiton efficiency is not markedly affected by the presence of CO_2. Therefore, the presence of CO_2-gas does not prevent the stabilization of the oxide film by polyol phosphate.

Fig. 4 shows Tafel diagrams obtained for AISI1020 carbon steel after 24 h of immersion in packer fluid and glyoxal, with and without inhibitor, with CO_2 bubbling. In the presence of inhibitor, reduction reactions are polarized (Eqs. (10), (11), and (12)), due probably to the blocking of cathodic sites by polyol phosphate adsorption. In anodic scanning, the passive zone current, in the presence of inhibitor, is smaller, but, after film breakage and pitting nucleation, the diagrams are similar.

Table 4 shows Tafel parameters obtained from the diagrams. E_{corr} values are more negative than those in the impedance experiments because scanning started at negative potentials. In view of the low-speed potential scanning, AISI 1020 carbon steel remained a while under cathodic polarization and may have occurred both reduction and thinning of the initial oxide film. The results corroborate those of the electrochemical impedance. In the absence of the inhibitor, the CO_2-containing medium presents greater current and smaller Tafel constants, whether anodic or cathodic, in this way showing depolarization of charge-transfer processes that occur through the metal/solution interface. With the addition of polyol phosphate-based inhibitor, corrosion current is diminished and Tafel constants are increased, pointing to the presence of an oxide film with adsorbed inhibitor that protects the steel. In the presence of dissolved CO_2, the current resumes its growth and Tafel constants are decreased, but not in the same order of magnitude as in the medium with CO_2 and without inhibitor. Therefore, the inhibitor hinders the corrosion of AISI 1020 carbon steel, even in the presence of CO_2.

Fig. 5 shows the images obtained from Scanning Electron Microscopy (SEM) for AISI 1020 carbon steel after 24 h of immersion time in packer fluid and glyoxal mixture and CO_2 bubbling, with and without inhibitor. In the absence of inhibitor, the carbon steel exhibits a surface covered with white crystals deposits. The images confirm that the iron undergoes oxidation in packer fluid and glyoxal solution and, in the presence of carbonate, yields corrosion products such as $FeCO_3$, porous and non-protective, as indicated by the electrochemical impedance parameters (Fig. 3). In the presence of inhibitor, the surface is more homogeneous, without corrosion products deposited. The coupon surface is smooth, showing polishing lines [50, 51]. A thin layer of oxide already existent on the surface of iron is stabilized by the corrosion inhibitor, which forms a physical barrier against chloride action, in this way hindering both the

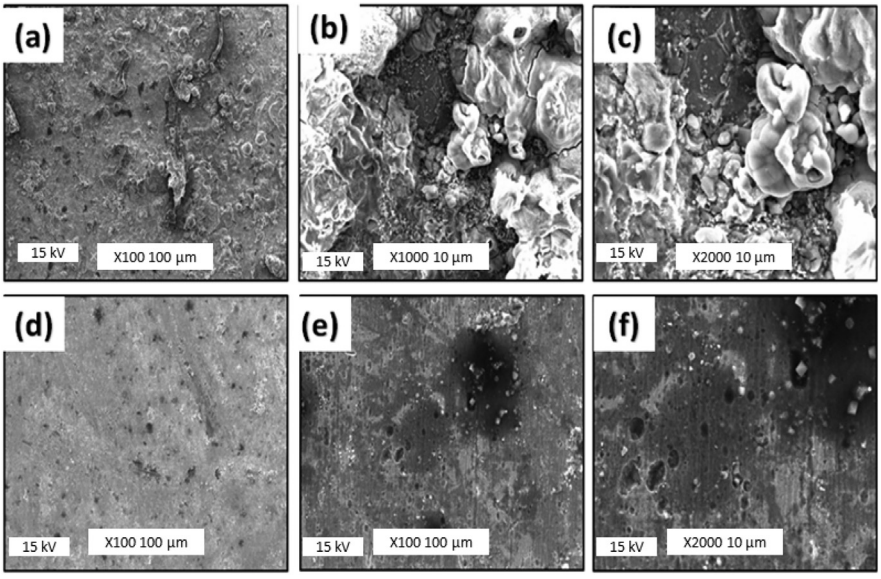

Fig. 5. SEM images for AISI 1020 carbon steel surface after 24 h of immersion in packer fluid (50 %) and glyoxal (50 %) mixtures without (5a, 5b and 5c) or with (5d, 5e and 5f) 500 ppm of polyol phosphate. Influence of CO_2.

oxidation and the formation of precipitates, derived from the solution saturation in the region close to the electrode. These images confirm the inhibiting action of polyol on carbon steel in packer fluid and glyoxal mixtures containing dissolved CO_2.

4. Conclusion

The corrosion inhibition efficiency of 1020 carbon steel in packer fluid and glyoxal mixtures, 50 % v/v, by polyol phosphate, obtained from renewable and environmentally friendly sources was investigated with the purpose of enabling the utilization of glyoxal as a mitigator of H_2S-gas coming from oil fields. The proposed inhibitor presents strong adsorption on the previous oxide, acting as a physical barrier between the metal and the solution.

Polyol phosphate with 10% H_3PO_4 exerted better control over corrosion than polyol with 2.5% H_3PO_4. The content of P groups (or phosphate anions) interferes directly in the inhibiting efficiency of polyol, resulting in greater polarization resistance, smaller capacitance and greater coverage degree, in this way evidencing that these groups promote stabilization of the iron oxide film through chemical adsorption, by means of oxygen bonds (bonded to phosphorus) and the oxygen vacancies of the defective oxide film.

The presence of CO_2-gas enhances the corrosion of AISI 1020 carbon steel in packer fluid and glyoxal, as verified by the impedance tests, by the decrease in polarization resistance and increase in capacitance, if compared with the medium without CO_2.. This effect is due to pH decrease and the consequent porous, non-protective $FeCO_3$ formation. The addition of inhibitor to the system promotes corrosion control. Therefore, the presence of CO_2-gas does not prevent polyol phosphate from stabilizing the oxide film. Polyol phosphate inhibits the corrosion caused by CO_2 present in petroleum when using media with packer fluid and glyoxal mixtures. SEM images confirm the deposition of corrosion products in CO_2-containing medium, which are absent in the presence of the inhibitor.

Declarations

Author contribution statement

Rita C. da Silva, Gabriel A. Lorenzi: Performed the experiments; Analyzed and interpreted the data.

Melissa Heinen, Demétrius W. Lima: Contributed reagents, materials, analysis tools or data.

João H. L. Moura: Analyzed and interpreted the data; Wrote the paper.

Jamili M. de Freitas: Performed the experiments.

Emilse M. A. Martini, Cesar L. Petzhold: Conceived and designed the experiments; Analyzed and interpreted the data; Wrote the paper.

Funding statement

This work was supported by the Conselho Nacional de Desenvolvimento Científico e Tecnológico (CNPq, Project nr. 405941/2016–1) and the Coordenação de Aperfeiçoamento de Pessoal de Nível Superior (CAPES - Financial Code 001).

Competing interest statement

The authors declare no conflict of interest.

Additional information

No additional information is available for this paper.

References

[1] I.B. Obot, D.D. Macdonald, Z.M. Gasem, Density functional theory (DFT) as a powerful tool for designing new organic corrosion inhibitors. Part 1: an overview, Corros. Sci. 99 (2015) 1–30.
[2] D. Wang, E. Sikora, B. Shaw, A study of the effects of filler particles on the degradation mechanisms of powder epoxy novolac coating systems under corrosion and erosion, Prog. Org. Coating 121 (2018) 97–104.
[3] S. Mohammed, G.A. Mansoori, The role of supercritical/dense CO2 gas in altering aqueous/oil interfacial properties: a molecular dynamics study, Energy Fuels 32 (2018) 2095–2103.
[4] A. Elias Jr., O.V. Trevisan, An experimental investigation on phase behavior of a light oil and CO_2, J. Pet. Sci. Eng. 145 (2016) 22–33.
[5] A. Benchikh, R. Aitout, L. Makhloufi, L. Benhaddad, B. Saidani, Soluble conducting poly(aniline-co-orthotoluidine) copolymer as corrosion inhibitor for carbon steel in 3% NaCl solution, Desalination 249 (2009) 466–474.
[6] J.M. Formigli, A.C.C. Pinto, A.S. Almeida, Santos basin's pre-salt reservoirs development: the way ahead, in: Offshore Technology Conference, OTC 19.953. Houston, Texas, 2009, https://doi.org/10.4043/19953-MS.
[7] G. Gabetta, S. Correra, S. Sgorlon, M. Bestetti, Test conditions for pipeline materials selection with high pressure sour gas, Int. J. Corros. (2018) 1–9.
[8] S. Nesic, Key issues related to modelling of internal corrosion of oil and gas pipelines – a review, Corros. Sci. 49 (2007) 4308–4338.
[9] A.S.G. Carvalho, L.F. De Ros, Diagenesis of aptian sandstone sand conglomerates of the campos basin, J. Pet. Sci. Eng. 125 (2015) 189–200.
[10] N.V. Likhanova, N. Nava, O. Olivares-Xometl, M.A. Domínguez-Aguilar, P. Arellanes-Lozada, I.V. Lijanova, L. Lartundo-Rojas, Corrosion evaluation of pipeline steel API 5L X52 in partially deaerated produced water with high chloride content, Int. J. Electrochem. Sci 13 (2018) 7949–7967.
[11] P. Xu, Z. Tao, Z. Wang, Corrosion-resistant systems of formate packer fluid for G3/N80/TP110SS pipes at high temperature, high pressure and high H_2S/CO_2 ratios, Royal Soc. Open Sci 5 (2018) 180405.
[12] L. Zea, P. Jepson, R. Kumar, Role of Pressure and Reaction Time on Corrosion Control of H_2S Scavenger, in: Department of Mechanical, Materials and Aerospace Engineering, University of Central Florida, SPE International Oilfield Corrosion Conference, Aberdeen, UK, 2008.
[13] E. Alibakhshi, M. Ramezanzadeh, G. Bahlakeh, B. Ramezanzadeh, M. Mahdavian, M. Motamedi, Glycyrrhiza glabra leaves extract as a green corrosion inhibitor for mild steel in 1 M hydrochloric acid solution: experimental, molecular, dynamics, Monte Carlo and quantum mechanics study, J. Mol. Liq. 255 (2018) 185–198.
[14] N. Asadi, M. Ranezanzadeh, G. Bahlakeh, B. Ramezanzadeh, Utilizing Lemon Balm extract as an effective green corrosion inhibitor for mild steel in 1 M HCl solution: a detailed experimental, molecular dynamics, Monte Carlo and quantum mechanics study, J Taiwan Inst. Chem. E. 95 (2019) 252–272.
[15] E. Alibakhsh, M. Ramezanzadeh, S.A. Haddadi, G. Bahlakeh, B. Ramezanzadeh, M. Mahdavian, Persian Liquorice extract as a highly efficient sustainable corrosion inhibitor for mild steel in sodium chloride solution, J. Clean. Prod. 210 (2019) 660–672.
[16] A. Deghani, G. Bahlakeh, B. Ramezanzadeh, M. Ranezanzadeh, Potential of Borage flower aqueous extract as an environmentally sustainable corrosion inhibitor for acid corrosion of mild steel: electrochemical and theoretical studies, J. Mol. Liq. 277 (2019) 895–911.
[17] Z. Sanaei, M. Ranezanzadeh, G. Bahlakeh, B. Ramezanzadeh, Use of Rosa Canina fruit extract as a green corrosion inhinitor for mild steel in 1 M HCl solution: a complementary experimental, molecular dynamics and quantum mechanics investigation, J. Ind. Eng. Chem. 69 (2019) 18–31.
[18] M. Ranezanzadeh, G. Bahlakeh, Z. Sanaei, B. Ramezanzadeh, Corrosion inhibitor of mild steel in 1 M HCl solution by ethanolic extract of eco-friendly Mangifera Indica (mango) leaves: electrochemical, molecular dynamics, Monte Carlo and ab initio study, Appl. Surf. Sci. 436 (2019) 1058–1077.
[19] P.C. Okafor, X. Liu, Y.G. Zheng, Corrosion inhibition of mild steel byethylaminoimidazoline derivative in CO_2-saturated solution, Corros. Sci. 51 (2009) 761–768.
[20] G. Salinas-Solano, J. Porcayo-Calderon, L.M. de la Escalera, J. Canto, M. Casales-Diaz, O. Sotelo-Mazon, L. Martinez-Gomez, Development and evaluation of a green corrosion inhibitor based on rice bran oil obtained from agro-industrial waste, J. Ind Crops Prod. 119 (2018) 111–124.
[21] Z.N. Yang, Y.W. Liu, Y. Chen, Linseed oil based amide as corrosion inhibitor for mild steel in hydrochloric acid, Int. J. Electrochem. Sci. 13 (2018) 514–529.
[22] M. Zouarhi, M. Chellouli, S. Abbout, H. Hammouch, A. Dermaj, S.O. Said Hassane, A. Srhiri, Inhibiting effect of a green corrosion inhibitor containing jatropha curcas seeds oil for iron in an acidic medium, Port. Electrochim. Acta 36 (2018) 179–195.
[23] A. Agi, R. Junin, M. Rasol, A. Gbadamosi, R. Gunaji, Treated Rhizophora mucronata tannin as a corrosion inhibitor in chloride solution, PLoS One 13 (2018), e0200595.
[24] A. Espinoza-Vazquez, F.J.R. Gomez, E. Juaristi, M. Escudero-Casao, G.E. Negron-Silva, D. Angeles-Beltran, M. Palomar-Pardave, β-Amino acid-derived triazols as corrosion inhibitors for API 5L X52 steel immersed in 1 M HCl, Int. J. Electrochem. Sci. 13 (2018) 7517–7531.
[25] J. Bao, H. Zhang, X. Zhao, J. Deng, Biomass polymeric microspheres containing aldehyde groups: immobilizing and controlled-releasing amino acids as green metal corrosion inhibitor, Chem. Eng. J. 341 (2018) 146–156.
[26] K. Zhang, W. Yang, X. Yin, Y. Chen, Y. Liu, J. Le, B. Xu, Amino acids modified konjac glucomannan as green corrosion inhibitors for mild steel in HCl solution, Carbohydr. Polym. 181 (2018) 191–199.

[27] A.A. Farag, A.S. Ismail, M.A. Migahed, Environmental-friendly shrimp waste protein corrosion inhibitor for carbon steel in 1 M HCl solution, Egypt. J. Petrol. 27 (4) (2018) 1187–1194.
[28] M. Bobina, A. Kellenberger, J.P. Millet, C. Muntean, N. Vaszilcsin, Corrosion resistance of carbon steel in weak acid solutions in the presence of l-histidine as corrosion inhibitor, Corros. Sci. 69 (2013) 389–395.
[29] E.E. Oguzie, Evaluation of the inhibitive effect of some plant extracts on the acid corrosion of mild steel, Corros. Sci. 50 (2008) 2993–2998.
[30] S. Ghareba, S. Omanovic, 12-Aminododecanoic acid as a corrosion inhibitor for carbon steel, Electrochim. Acta 56 (2011) 3890–3898.
[31] J. Sun, C. Sun, G. Zhang, X. Li, W. Zhao, T. Jiang, H. Liu, X. Cheng, Y. Wang, Effect of O_2 and H_2S impurities on the corrosion behavior of X65 steel in water-saturated supercritical CO_2 system, Corros. Sci. 107 (2016) 31–40.
[32] P. Han, C. Chen, H. Yu, Y. Xu, Y. Zheng, Study of pitting corrosion of L245 steel in H_2S environments induced by imidazoline quaternary ammonium salts, Corros. Sci. 112 (2016) 128–137.
[33] S. Saker, N. Aliouane, H. Hammache, S. Chafaa, S. Chafaa, G. Bouet, Tetraphosphonic acid as eco-friendly corrosion inhibitor on carbon steel in 3 % NaCl aqueous solution, Ionics 21 (2015) 2079–2090.
[34] N. Srisuwan, N. Ochoa, N. Pébére, B. Tribollet, Variation of carbon steel corrosion rate with flow conditions in the presence of an inhibitive formulation, Corros. Sci. 50 (2008) 1245–1250.
[35] N. Ochoa, F. Moran, N. Pébére, B. Tribollet, Influence of flow on the corrosion inhibition of carbon steel by fatty amines in association with phosphonocarboxylic acid salts, Corros. Sci. 47 (2005) 593–604.
[36] Z. Shen, H. Ren, K. Xu, J. Geng, L. Ding, Inhibition effect of phosphorus-based chemicals on corrosion of carbon steel in secondary-treated municipal wastewater, Water Sci. Technol. 67 (2013) 2412–2417.
[37] N. Ochoa, G. Baril, F. Moran, N. Pébère, Study of the properties of a multi-component inhibitor used for water treatment in cooling circuits, J. Appl. Electrochem. 32 (2002) 497–504.
[38] H. Amar, J. Benzakour, A. Derja, D. Villemin, B. Moreau, T. Braisaz, Piperidin-1-yl-phosphonic acid and (4-phosphono-piperazin-1-yl) phosphonic acid - a new class of iron corrosion inhibitors in NaCl 3%, Appl. Surf. Sci. 252 (2006) 6162–6172.
[39] L. Cáceres, T. Vargas, M. Parra, Study of the variational patterns for corrosion kinetics of carbon steel as a function of dissolved oxygen and NaCl concentration, Electrochim. Acta 54 (2009) 7435–7443.
[40] N. Nakayama, Inhibitory effects of nitrilotris(methylenephosphonic) acid on cathodic reactions on steels in saturated $Ca(OH)_2$ solutions, Corros. Sci. 42 (2000) 1897–1920.
[41] I. Felhosi, J. Telegdi, G. Pálinkás, E. Kálmán, Kinetics of self-assembled layer formation on iron, Electrochim. Acta 47 (2002) 2335–2340.
[42] M. Mobin, S. Zehra, M. Parveen, l-Cysteine as corrosion inhibitor for mild steelin 1 M HCl and synergistic effect of anionic, cationic and non-ionic surfactants, J. Mol. Liq. 216 (2016) 598–607.
[43] R.C. Silva, M. Heinen, G.A. Lorenzi, C.L. Petzhold, E.M.A. Martini, Vegetable polyol phosphate as corrosion inhibitor of carbon steel in packer fluid solutions, Ionics 23 (6) (2017) 1569–1578.
[44] M. Heinen, A.E. Gerbase, C.L. Petzhold, Vegetable oil-based rigid polyurethanes and phosphorylated flame-retardants derived from epoxydized soybean oil, Polym. Degrad. Stabil. 108 (2014) 76–86.
[45] J.P. Simpson, Stability and Corrosivity of Packer Fluids, American Petroleum Institute, 1968, pp. 46–52. API-68-046.
[46] T. Tuken, F. Demir, N. Kicir, G. Sigircik, M. Erbil, Inhibition effect of 1-Ethyl-3-methyl-imidazolium dicyanamide against steel corrosion, Corros. Sci 59 (2012) 110–118.
[47] Q.L. Liu, L.I. Mao, S.W. Zhou, Effects of chloride content on CO_2 corrosion of carbon steel in simulated oil and gas wel environments, Corros. Sci. 84 (2014) 165–171.
[48] C. Su, J. Sun, Y. Wang, X. Liu, X. Li, X. Cheng, H. Liu, Synergistic effect of O_2, H_2S and SO_2 impurities on the corrosion behavior of X65 steel in water-saturated supercritical CO_2 system, Corros. Sci 107 (2016) 193–203.
[49] M. Askari, M. Aliofkhazraei, S. Ghaffari, A. Hajizadeh, Film former corrosion inhibitors for oil and gas pipelines-A technical review, J. Nat. Gas Sci. Eng. 58 (2018) 92–114.
[50] H. Liu, T. Gu, Y. Lv, M. Asif, F. Xiong, G. Zhang, H. Liu, Corrosion inhibition and anti-bacterial efficacy of benzalkonium chloride in artificial CO_2-saturated oilfield produced water, Corros. Sci. 117 (2017) 24–34.
[51] H. Tian, W. Li, B. Hou, D. Wang, Insights into corrosion inhibition of multi-active compounds for X65 pipeline steel in acidic oilfield formation water, Corros. Sci. 117 (2017) 43–58.